A tandem photoelectrochemical cell based on Cu2-xTe nanocrystals for solar energy conversion to hydrogen

A Tandem Photoelectrochemical Cell Based on $Cu_{2-x}Te$ Nanocrystals for Solar Energy Conversion to Hydrogen

Elena Alfonso-González (a), Marta Liras (a), Mengjiao Wang (b), Ignacio J. Villar-García (a, c), Luca de Trizio (b), Mariam Barawi (a) and Víctor A. de la Peña O´Shea* (a)*

(a) Photoactivated Processes Unit, IMDEA Energy Institute, Avda. Ramón de la Sagra, 3. 28935 Móstoles (Madrid) Spain.

(b) Nanochemistry Department, Istituto Italiano di Tecnologia, Via Morego 30, 16163 Genova, Italy.

(c) Present address: ALBA Synchrotron, Carrer de la Llum 2-26, 08290 Cerdanyola del Vallès (Barcelona) Spain.

Corresponding Authors

Mariam Barawi: mariam.barawi@imdea.org

Víctor A. de la Peña O´Shea: victor.delapenya@imdea.org

ABSTRACT

In this work we present the design, assembly and characterization of a tandem photoelectrochemical (PEC) cell based on two different crystallographic phases of sub-stoichiometric copper telluride nanocrystals (NCs). The first one, a pseudo-cubic phase, pc-$Cu_{2-x}Te$, is characterized by positive photocurrents, whilst the second one, a hexagonal phase, h-$Cu_{2-x}Te$, favors negative ones. We have taken advantage of these differences in their optoelectronic properties to prepare a hybrid pc-$Cu_{2-x}Te/TiO_2$ photoanode, with TiO_2 acting as light absorber and electron scavenger, and a h-$Cu_{2-x}Te$/CuI photocathode, with CuI behaving as photoabsorber and hole scavenger. The tandem PEC cell shows a photocurrent density of ~0.5 mA/cm^2 when measured in a 2-electrode configuration without any co-catalyst. Finally, to test the PEC cell perform the hydrogen evolution reaction (HER) a thin film of Pt was deposited on top of the photocathode, and ~7 µmol of hydrogen were obtained at 0.6 V in a one-hour experiment, reaching a photocurrent of 1 mA/cm^2. The cell exhibits a great photostability showing no loss in photocurrent during the one-hour reaction.

TOC GRAPHICS

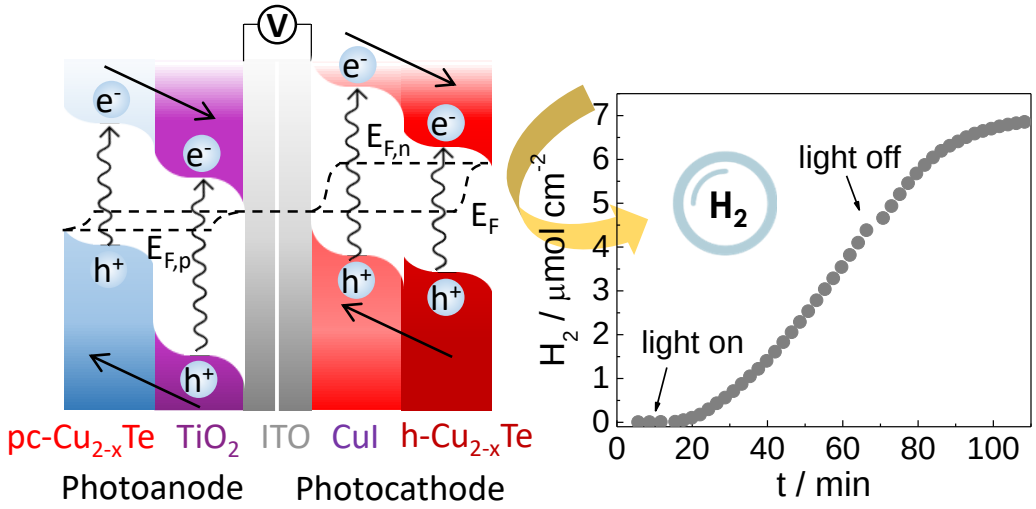

Looking into the ever-increasing global energy demands and the undesirable environmental impacts of fossil fuels, solar energy emerges as an alternative source because of its abundant and renewable nature. While the conversion of such energy into electricity *via* solar cells is a highly studied and efficient process, the storage of the generated electric energy remains a bottleneck due to the lack of efficient accumulators/batteries. A direct use of the solar energy to obtain fuels via artificial photosynthesis (AP) is a very promising approach.[1] In this context, photoelectrochemical (PEC) cells are one of the most attractive technologies, as they have led to some of the highest solar-to-hydrogen efficiencies achieved to date.[2] From the materials point of view, there are different strategies that have been addressed so far to improve their efficiency, such as semiconductor doping, nanostructuring and the use of multinary oxides or smaller band gap materials such as some metal chalcogenides like CuSe, PbSe or HgSe.[1,3–5] From the fabrication point of view, advanced inorganic colloidal nanocrystal approaches to produce homogenous inks are some of the most interesting strategies to design efficient photoelectrodes. These synthetic approaches allow obtaining a huge number of multifunctional and versatile materials with a high control of the size, shape, composition, dispersion, and surface termination. All these features govern their optoelectronic properties and consequently, their use as building-electrode materials for PEC cells.

Many colloidal systems have been studied to prepare photoelectrodes, with metal oxides being the most commonly used materials.[5–8] Metal chalcogenides exhibit several advantages compared to metal oxides. In general, they have higher conduction band edge positions, smaller band gap energy and greater conductivities.[6,9,10] Among them, CdS and CdSe are some of the most active materials for photocatalytic applications.[6,9] However, their low stability towards corrosion and the toxic and carcinogenic nature of cadmium

represent a considerable hurdle for their widespread application. Consequently, other non-toxic and more stable metal chalcogenides are investigated as alternatives for HER in PEC systems.[11]

Over the past few years, vacancy-doped semiconductors, such as copper chalcogenides, $Cu_{2-x}Y$ (Y = S, Se, Te), have generated much interest on photovoltaic, photonic and electrocatalytic applications due to their interesting opto-electronic properties and the high abundance of copper.[10,12,13] In these materials, copper vacancies lead to an increase in the charge carrier density (up to 10^{21} cm^{-3}).[12] These sub-stoichiometric systems also present a strong plasmonic response, which is explained by the existence of a 3D connected vacancy channel system.[12] Moreover, as Te is less electronegative than S and Se, $Cu_{2-x}Te$ compounds are characterized by the lowest ionic character of the Cu-Y bonds among the $Cu_{2-x}Y$ materials, which provides it with a larger carrier mobility.[10] However, as far as we know, pc-Cu2-xTe has not been used despite its potential as photoelectrode material. Several authors have shown a relationship between optical and electronic properties, such as band gap, conductivity, mobility and carrier concentration, with structural ones.[14,15] In fact, among the possible crystal phases hexagonal $Cu_{2-x}Te$ has been recently studied as an electrocatalyst for HER, showing a low overpotential, very low charge transfer resistance, R_{ct}, and long-term stability.[13] Furthermore, the use of colloidal synthesis tools lead to novel structures with interesting photo(electro) catalytic properties.

Motivated by these promising features, we explore in this work the possibility of tuning the structural properties of these two $Cu_{2-x}Te$ phases in order to change their electronic band positions and favor either positive or negative photocurrents. In a second step, we use the optimized $Cu_{2-x}Te$ phases to construct a tandem PEC cell for HER with h-$Cu_{2-x}Te$ as the photoanode and pc-$Cu_{2-x}Te$ as the photocathode.

Structural and electronic properties.

Colloidal pc-$Cu_{2-x}Te$ nanocubes (Figure 1a) where synthetized using a microemulsion method, based on the use of specific ligands as surfactants.[12] This phase presents an unusual pseudo-cubic structure (see Figure 1b) characterized by the presence of Cu vacancies. DFT calculations (Figure 1c) were used to predict the electronic structure and an estimated band gap of 1.68 eV was found. The electronic densities of states (DOS) of the pc-$Cu_{2-x}Te$ phase shows a valence band minimum (VBM) and a conduction band maximum (CBM) mainly composed of Cu 3d and Te 5d states. The presence of Cu vacancies leads to the appearance of electronic states above E_F. In addition, the electronic localization function (ELF) allocates an increase on the electron density in the Te atoms with lower coordination (Figure 1d).

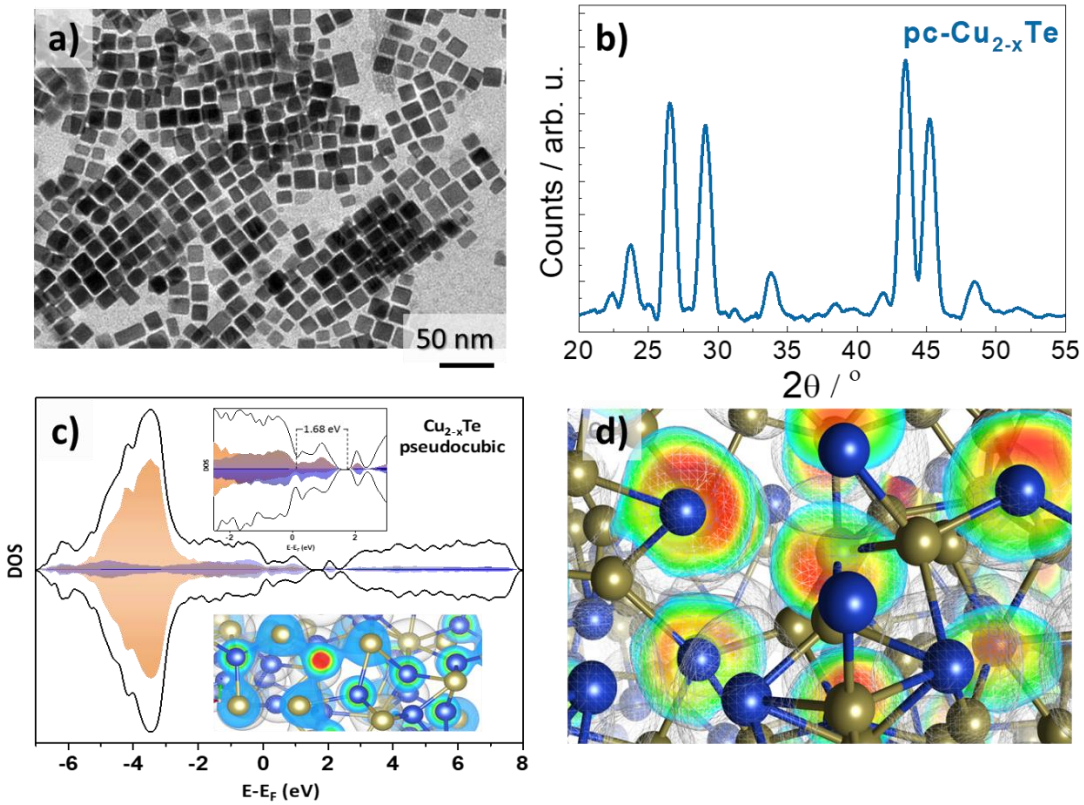

Figure 1. a) TEM image of pc-$Cu_{2-x}Te$ NCs nanocubes, b) XRD diffractograms c) Projected Cu 3d (orange) and Te 5p (blue) density of states (DOS) and valence band (VB)

magnification (inset) and d) Electronic localization function (ELF) of $Cu_{2-x}Te$ pseudo-cubic phase pc-$Cu_{2-x}Te$. Atom color: Cu (gold) and Te (blue).

In order to prepare the photoelectrodes, the colloidal solution ($Cu_{2-x}Te$ NCs dispersed in hexane, details in SI) was deposited on ITO (Indium Tin Oxide) coated glass by drop casting (see details in SI). Previously, a ligand exchange method with mercaptopropionic acid was used in order to remove the primitive organic capping present in the as-synthesized phase and to enhance the conductivity of the NCs thin films. The removal of the organic capping was monitored by FTIR (figure S1) and the effect over the conductivity performance with a ligand or other by Electrochemical Impedance Spectroscopy (EIS) experiments (Figure S2 and table S1)

In addition, we performed a thermal treatment of the pc-$Cu_{2-x}Te$ photoelectrodes thin films in order to prepare the hexagonal crystal phase h-$Cu_{2-x}Te$. To do that, we carried out a phase change study in which we monitored via High Temperature X-Ray Diffraction (HT-XRD) the evolution of the crystal structure during an annealing treatment from 25°C to 500°C under an argon mixture of crystallographic phases started to appear at 300 °C and a pure hexagonal atmosphere (Figure S3) observing the hexagonal $Cu_{2-x}Te$ phase appears at 425 °C. Moreover, after all the chemical and thermal treatments, we performed a XPS analysis to verify if copper telluride remains not only in the bulk but also on the photoelectrodes surface. Cu 2p3/2 and Te 3d5/2 XPS spectra in figure S5 exhibit that the photoelectrodes surface is mainly composed by CuTe compounds in all cases, with an amount of oxide peaks being somewhat larger, as expected, for the case of the sintered sample at higher temperature, h-$Cu_{2-x}Te$.

In order to investigate the influence of crystalline-structure changes into the optoelectronic structure of pc-$Cu_{2-x}Te$, we perform an optical, electronic and photoelectrochemical characterization of both pure crystalline phases.

As expected, modifications in the crystal structure led to changes in the optoelectronic properties,[14,15] which will play an important role in their behavior as photoelectrodes. Optical band gap energies were determined by means of UV-Vis-NIR transmittance and reflectance spectroscopy (figure S6). In this sense, the absorption coefficient was calculated (SI equation 1) and the corresponding Tauc plots build. As can be seen in figure 2a and b, two direct transitions of 1.66 eV for h-$Cu_{2-x}Te$ and 1.67 eV for pc-$Cu_{2-x}Te$ were found, which is in accordance with DFT studies (Figure 1). The electronic band structure of both $Cu_{2-x}Te$ phases was experimentally obtained by the combination of several characterization techniques. Valence band (VB) energy determined by XPS is 0.11±0.02 and 0.33±0.02 eV for the pseudo-cubic and hexagonal phases respectively (Figure 2 c and d). These low values in comparison to the band gap energy, are characteristic of p-type semiconductors, which is expected due to copper vacancies within the lattice.[10] Flat band potentials (V_{fb}), from which the Fermi level energy can be directly obtained,[16] are -0.18±0.02 and -0.12±0.02 $V_{Ag/AgCl}$ at pH=9 for pseudo-cubic and hexagonal phases respectively, as measured by linear sweep voltammetry (LSV) under dark and light conditions (figure S7). Additionally, chronoamperometries at different bias potential confirm the photocurrent sign change (figure S8) and the ability of this material to be used as photoelectrodes. We observe that p-$Cu_{2-x}Te$ has a more negative V_{fb} than h-$Cu_{2-x}Te$. The electronic structure obtained for both phases (figure 1 d) suggests that both materials are suitable to be part of a tandem cell for HER as the conduction band energy edges are more energetic than the redox par responsible of the water reduction (see figure 2e).

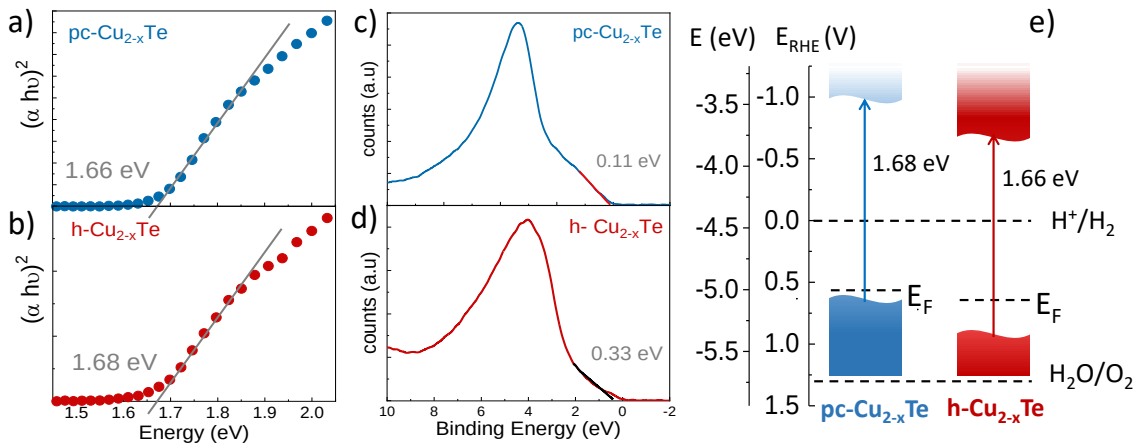

Figure 2. a, b) Tauc plots obtained by UV-Vis Spectroscopy, c-d) XPS valence band spectra and e) electronic band diagram of pc-$Cu_{2-x}Te$ (blue) and h-$Cu_{2-x}Te$ (red).

Photocurrents of both phases were then more thoroughly investigated at different bias potentials by chronoamperometries under chopped AM 1.5G illumination. Figure 3a and 3b display the cathodic measurements, whereas figure 3c and d the anodic ones. Part d of this figure exhibits the acquired photocurrents obtained at the different applied potentials. Interestingly, these measurements reveal that the h-$Cu_{2-x}Te$ phase offers higher positive photocurrents than the pc-$Cu_{2-x}Te$ phase, while the h-$Cu_{2-x}Te$ phase shows higher negative photocurrents than the pc-$Cu_{2-x}Te$ phase.

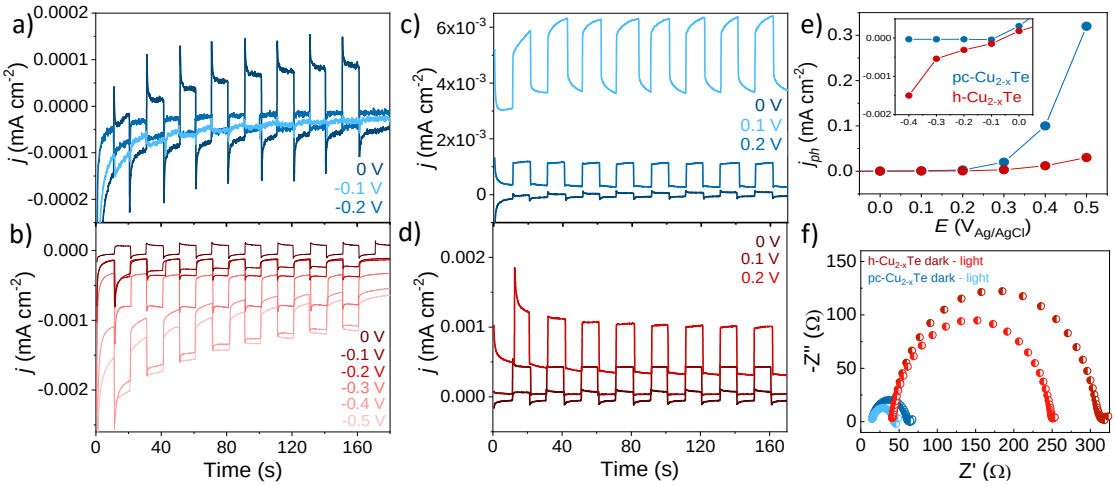

Figure 3. a-d) Chronoamperometries under chopped illumination at different bias potentials (V vs Ag/AgCl) of pc-$Cu_{2-x}Te$ (blue, a and c) and h-$Cu_{2-x}Te$ (red, b and d). e) Extracted photocurrents and f) Nyquist plot under dark and illumination conditions at 0.5 V vs Ag/AgCl of both photoelectrodes.

Besides, in the chronoamperometries of figure 3a we can see a current drop in the photocurrent after illuminating the h-$Cu_{2-x}Te$ photoelectrode that can be attributed to recombination and cannot be observed in pc-$Cu_{2-x}Te$ (just in the first transient at 0.2V). In this sense, EIS experiments were carried out to deeply investigate the charge transfer across the $Cu_{2-x}Te$/electrolyte interface (see Nyquist plot in figure 2f). By fitting the Nyquist plot, the equivalent electrical circuit was obtained. R_{ct} is the resistance associated with the electronic transport through the semiconductor-electrolyte interface. Its calculated values show better conductivity in pc-$Cu_{2-x}Te$ compared to h-$Cu_{2-x}Te$ (table S1). This could account for the recombination observed in figure 2 c). R_{ct} decreases considerably under bias potential and illumination conditions, demonstrating the ability of these materials to be used as photoelectrodes in solar energy conversion.

Monolithic Tandem PEC Cell Design, Characterization and H_2 Quantification

Taking all of these aspects into account, we designed a multilayer tandem PEC cell where the photoanode was comprised of TiO_2 anatase with pc-$Cu_{2-x}Te$ deposited on top. TiO_2 is a well-known semiconductor used in photoanodes due to its low cost, its very good chemical and optical stability and its potential to absorb a wider part of the solar spectrum when combined with other materials, as TiO_2 is unable to absorb the visible light.[17,18] On the other hand, for the h-$Cu_{2-x}Te$ based photocathode, we proposed the utilization of CuI, which is known to be a good hole scavenger to hinder the charge recombination exhibited

by h-$Cu_{2-x}Te$.[19–21] This configuration will allow to harvest a wide range of the solar spectrum from the UV to the visible light.

Before building the monolithic tandem PEC cell, each hybrid photoelectrode was characterized separately and compared to their single components in order to quantify possible and desired synergistic effects. The results acquired through linear sweep voltammetry (LSV) under chopped illumination depicted in figure 4a and b demonstrate that the photocurrents highly increase in the hybrid photoelectrodes when compared to the bare ones. On the one hand, the observed photocurrents are one and two orders of magnitude higher for the pc-$Cu_{2-x}Te/TiO_2$ hybrid photoelectrodes than for the bare TiO_2 or pc-$Cu_{2-x}Te$ ones respectively (figure 3 a) and not only in the photocurrent but also in the dark current density. On the other hand, we observe an improvement of three orders of magnitude in the photocurrent of the hybrid CuI/h-$Cu_{2-x}Te$ photocathode compared to the CuI and h-$Cu_{2-x}Te$ responses (figure 3b). This synergistic effect can be explained by the ability of CuI to hinder electron-hole recombination in h-$Cu_{2-x}Te$, even though we can still see recombination in figure 3b and S9. To confirm this behavior, we performed chronoamperometries at different bias potentials, demonstrating the improvement in light absorption and charge transfer in both photoelectrodes at stationary conditions (figure S11).

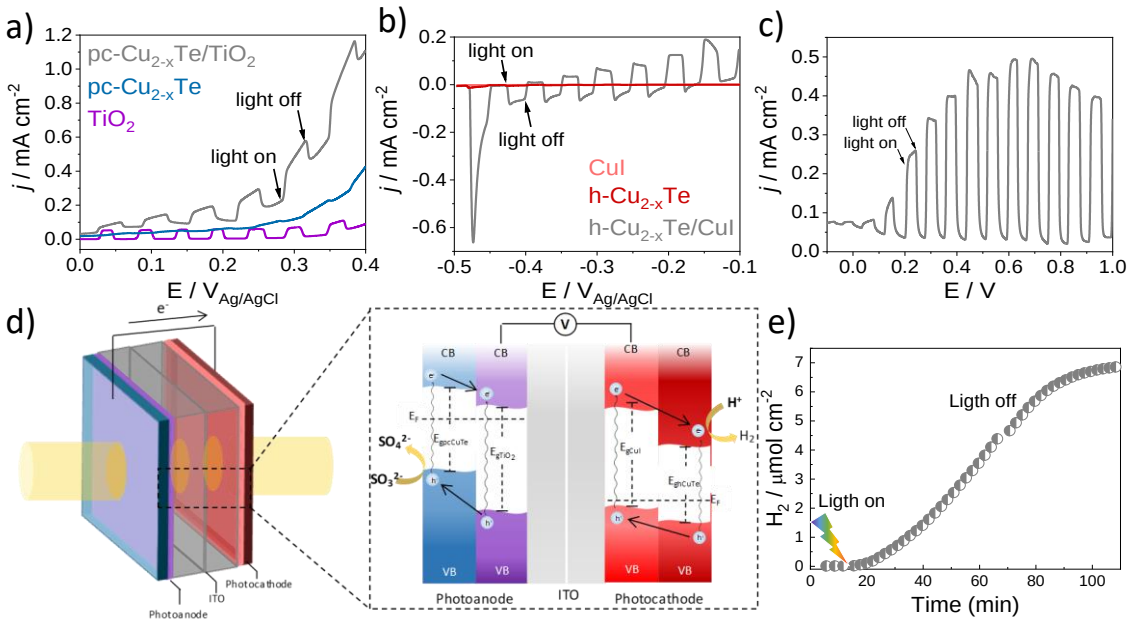

Figure 4. LSV under chopped AM1.5G illumination of the hybrid photoanode (a) and photocathode (b) compared to their separated components in a three-electrode configuration. LSV (c), scheme (d) and accumulated H_2 evolution at 0.6 V (e) of the monolithic tandem PEC cell in a two-electrode configuration under AM1.5G illumination.

Encouraged by these results, we built a monolithic tandem PEC cell (Figure 4d and S12) and measured the performance in both three- (figure S13) and two-electrode (Figure 4c) configurations. In this sense, results with three electrodes demonstrate that this cell has the potential to harvest the solar energy and transfer it to the external circuit. The recorded photocurrents are around 0.2 mA/cm^2 in a wide range of potential. In light of these results, we moved to a two-electrode configuration to understand the real potential difference between the two photoelectrodes and afterwards performed hydrogen evolution experiments. In figure 4c, the onset potential appears at -0.1 V, and photocurrents reach values of around 0.5 mA/cm^2 at 0.6 V. The HER experiments were preformed depositing a thin film of Pt (17 nm, see the AFM profile in figure S14) over the h-$Cu_{2-x}Te$ as co-

catalyst. The accumulated H_2 generated after one-hour of AM 1.5G irradiance was 7 μmol at 0.6 V (figure 3d) and the photocurrent reached 1 mA/cm^2 (figure S15).

To conclude, in this work we have successfully designed and built a tandem PEC cell, that covers the whole UV-VIS spectra by using two hybrid photoelectrodes based on vacant-doped copper telluride nanocrystals with different structural and optoelectronic properties. The photoanode was comprised by pc-$Cu_{2-x}Te$, which shows higher positive photocurrents, combined with TiO_2 as an electron scavenger. This hybrid photoanode shows an increase of one and two orders of magnitude in the photocurrent compared with the bare components. On the other hand, the photocathode is formed by h-$Cu_{2-x}Te$ combined with CuI as a hole scavenger, showing an enhancement of the photocurrents of three orders of magnitude with respect to the bare materials. This tandem cell exhibited a great photocurrent and stability during a one-hour H_2 evolution experiment and produced an amount of 7 μmol of H_2 with a photocurrent of 1 mA/cm^2.

ASSOCIATED CONTENT

Supporting information: experimental conditions; additional photoelectrochemical studies; AFM, XRD, FTIR and UV-VIS-NIR spectroscopy measurements; pictures of the PEC setup and the photoelectrodes.

AUTHOR INFORMATION

Corresponding Authors

Mariam Barawi: mariam.barawi@imdea.org

Víctor A. de la Peña O´Shea: victor.delapenya@imdea.org

ORCID

Elena Alfonso-González: 0000-0003-3639-6329

Marta Liras: 0000-0002-1724-1586

Ignacio J. Villar-García: 0000-0002-5657-5212

Mariam Barawi: 0000-0001-5719-9872

Víctor A. de la Peña O'Shea: 0000-0001-5762-4787

The authors declare no competing financial interest.

ACKNOWLEDGMENT

Financial support from the regional government of Comunidad de Madrid through FotoArt-CM project (S2018/NMT-4367) and Fundación Ramón Areces (Art-Leaf project). This work also received funding from the European Research Council (ERC) under the European Union's Horizon 2020 research and innovation program through the projects: HyMAP project, grant agreement No. 648319, ERC-2019-POC-Proof of Concept (NanoCPP) and the H2020-EU.1.2.2., FET Proactive program project Hysolchem. M.L. thanks the Spanish MINECO-AEI/ESF, UE the *Ramón y Cajal* grand (RyC-2015-18677). M.B. thanks the Spanish MINECO-AEI the *Juan de la Cierva Incorporación* grant (JC2019 – 042430 –I). We gratefully acknowledge Fernando Picó for the XRD measurements. The results reflect only the authors' view and the Agency is not responsible for any use that may be made of the information they contained.

REFERENCES

(1) Sivula, K.; van de Krol, R. Semiconducting Materials for Photoelectrochemical Energy Conversion. *Nat. Rev. Mater.* **2016**, *1*, 1–16. https://doi.org/10.1038/natrevmats.2015.10.

(2) Young, J. L.; Steiner, M. A.; Döscher, H.; France, R. M.; Turner, J. A.; Deutsch, T. G. Direct Solar-to-Hydrogen Conversion via Inverted Metamophic Multijunction Semiconductor Architectures. *Nat. Energy* **2017**, *2* (17028), 1–8. https://doi.org/10.1038/nenergy.2017.28.

(3) Yang, W.; Prabhakar, R. R.; Tan, J.; Tilley, S. D.; Moon, J. Strategies for Enhancing the Photocurrent, Photovoltage, and Stability of Photoelectrodes for Photoelectrochemical Water Splitting. *Chem. Soc. Rev.* **2019**, *48* (19), 4979–5015. https://doi.org/10.1039/c8cs00997j.

(4) Jian, J.; Jiang, G.; van de Krol, R.; Wei, B.; Wang, H. Recent Advances in Rational Engineering of Multinary Semiconductors for Photoelectrochemical Hydrogen Generation. *Nano Energy*. 2018. https://doi.org/10.1016/j.nanoen.2018.06.074.

(5) van de Krol, R.; Grätzel, M. *Photoelectrochemical Hydrogen Production*; 2012. https://doi.org/10.1007/978-1-4614-1380-6.

(6) Sivula, K.; Prevot, M. S. Photoelectrochemical Tandem Cells for Solar Water Splitting. *J. Phys. Chem. C* **2013**, *117*, 17879–17893.

(7) Xie, G.; Zhang, K.; Guo, B.; Liu, Q.; Fang, L.; Gong, J. R. Graphene-Based Materials for Hydrogen Generation from Light-Driven Water Splitting. *Adv. Mater.* **2013**, *25* (28), 3820–3839. https://doi.org/10.1002/adma.201301207.

(8) Naldoni, A.; Montini, T.; Malara, F.; Mróz, M. M.; Beltram, A.; Virgili, T.; Boldrini, C. L.; Marelli, M.; Romero-Ocaña, I.; Delgado, J. J.; Dal Santo, V.; Fornasiero, P. Hot Electron Collection on Brookite Nanorods Lateral Facets for Plasmon-Enhanced Water Oxidation. *ACS Catal.* **2017**, 1270–1278. https://doi.org/10.1021/acscatal.6b03092.

(9) Tee, S. Y.; Win, K. Y.; Teo, W. S.; Koh, L.-D.; Liu, S.; Teng, C. P.; Han, M.-Y. Recent Progress in Energy-Driven Water Splitting. *Adv. Sci.* **2017**, 1600337. https://doi.org/10.1002/advs.201600337.

(10) Coughlan, C.; Ibáñez, M.; Dobrozhan, O.; Singh, A.; Cabot, A.; Ryan, K. M. Compound Copper Chalcogenide Nanocrystals. *Chem. Rev.* **2017**, *117* (9), 5865–6109. https://doi.org/10.1021/acs.chemrev.6b00376.

(11) Barawi, M.; Flores, E.; Ferrer, I. J.; Ares, J. R.; Sánchez, C. Titanium Trisulphide (TiS 3) Nanoribbons for Easy Hydrogen Photogeneration under Visible Light. *J. Mater. Chem. A* **2015**, *3* (15), 7959–7965. https://doi.org/10.1039/C5TA00192G.

(12) Mugnaioli, E.; Gemmi, M.; Tu, R.; David, J.; Bertoni, G.; Gaspari, R.; De Trizio, L.; Manna, L. Ab Initio Structure Determination of Cu2- XTe Plasmonic Nanocrystals by Precession-Assisted Electron Diffraction Tomography and HAADF-STEM Imaging. *Inorg. Chem.* **2018**, *57* (16), 10241–10248. https://doi.org/10.1021/acs.inorgchem.8b01445.

(13) Kumaravel, S.; Karthick, K.; Thiruvengetam, P.; Johny, J. M.; Sankar, S. S.; Kundu, S. Tuning Cu Overvoltage for a Copper-Telluride System in Electrocatalytic Water Reduction and Feasible Feedstock Conversion: A New Approach. *Inorg. Chem.* **2020**, *59* (15), 11129–11141. https://doi.org/10.1021/acs.inorgchem.0c01648.

(14) Yu, L.; Luo, K.; Chen, S.; Duan, C. G. Cu-Deficiency Induced Structural Transition of Cu2-XTe. *CrystEngComm* **2015**, *17* (14), 2878–2885. https://doi.org/10.1039/c4ce02370f.

(15) Salmón-Gamboa, J. U.; Barajas-Aguilar, A. H.; Ruiz-Ortega, L. I.; Garay-Tapia,

A. M.; Jiménez-Sandoval, S. J. Vibrational and Electrical Properties of Cu2-XTe Films: Experimental Data and First Principle Calculations. *Sci. Rep.* **2018**, *8* (1), 1–12. https://doi.org/10.1038/s41598-018-26461-x.

(16) Cardon, F.; Gomes, W. P. On the Determination of the Flat-Band Potential of a Semiconductor in Contact with a Metal or an Electrolyte from the Mott-Schottky Plot. *J. Phys. D. Appl. Phys.* **1978**, *11* (4). https://doi.org/10.1088/0022-3727/11/4/003.

(17) Chen, X.; Zhang, Z.; Chi, L.; Nair, A. K.; Shangguan, W.; Jiang, Z. Recent Advances in Visible-Light-Driven Photoelectrochemical Water Splitting: Catalyst Nanostructures and Reaction Systems. *Nano-Micro Lett.* **2016**, *8* (1), 1–12. https://doi.org/10.1007/s40820-015-0063-3.

(18) Kalamaras, E.; Maroto-Valer, M. M.; Shao, M.; Xuan, J.; Wang, H. Solar Carbon Fuel via Photoelectrochemistry. *Catal. Today* **2018**, *317* (October 2017), 56–75. https://doi.org/10.1016/j.cattod.2018.02.045.

(19) Rojas, H. C.; Bellani, S.; Sarduy, E. A.; Fumagalli, F.; Mayer, M. T.; Schreier, M.; Grätzel, M.; Di Fonzo, F.; Antognazza, M. R. All Solution-Processed, Hybrid Organic-Inorganic Photocathode for Hydrogen Evolution. *ACS Omega* **2017**, *2* (7), 3424–3431. https://doi.org/10.1021/acsomega.7b00558.

(20) Christians, J. A.; Fung, R. C. M.; Kamat, P. V. An Inorganic Hole Conductor for Organo-Lead Halide Perovskite Solar Cells. Improved Hole Conductivity with Copper Iodide. *J. Am. Chem. Soc.* **2014**, *136*, 758–764. https://doi.org/10.1021/ja411014k.

(21) Rojas, H. C.; Bellani, S.; Fumagalli, F.; Tullii, G.; Leonardi, S.; Mayer, M. T.;

Schreier, M.; Grätzel, M.; Lanzani, G.; Di Fonzo, F.; Antognazza, M. R. Polymer-Based Photocathodes with a Solution-Processable Cuprous Iodide Anode Layer and a Polyethyleneimine Protective Coating. *Energy Environ. Sci.* **2016**, *9* (12), 3710–3723. https://doi.org/10.1039/c6ee01655c.

(22) Chen, Z.; Dinh, H. N.; Miller, E. *Photoelectrochemical Water Splitting*; 2013. https://doi.org/10.1007/978-1-4614-8298-7.